JOURNAL OF Applied Polymer SCIENCE

Electrical percolation behavior of carbon fiber and carbon nanotube polymer composite foams: Experimental and computational investigations

Alireza Foroozani Behbahani, Ghodratollah Hashemi Motlagh, Morteza Ziaee, Goolia Nikravan
School of Chemical Engineering, College of Engineering, University of Tehran, 16th Azar Avenue, Enqelab Street, P. O. Box 11155-4563, Tehran, Iran
Correspondence to: G. H. Motlagh (E-mail: ghmotlagh@ut.ac.ir)

ABSTRACT: The effect of foaming on the electrical percolation of polymer composites was simulated by a random sequential additional (RSA) process. Polystyrene composites containing various amounts of carbon fiber (CF) and carbon nanotubes (CNTs) were prepared through melt blending in an internal mixer and subsequently compression-molded to solid and foam sheets. The electrical conductivity (EC) and percolation threshold (P_c) of both the solid and foam composites were determined to evaluate the simulation results. The experimental results show that the EC of the CF composites decreased with foaming, whereas for the CNT composites, no significant change was observed. The RSA process was used to construct the microstructure of the solid and foam composites and predict their P_cs. Several parameters, including the fiber aspect ratio, bubble volume fraction, and bubble size, were studied by the simulation approach. The P_cs obtained by simulation showed good agreement with the experimental values. When bubbles were excluded to define the volume fraction of the filler, the foam composites with bubbles, close to the fibers in size, had approximately the same P_cs as the solid composites. Better agreement between the experimental and simulation results was found for the foam composites with 30 vol % bubbles rather than those with 15 vol %. © 2015 Wiley Periodicals, Inc. J. Appl. Polym. Sci. **2015**, *132*, 42685.

KEYWORDS: composites; fibers; foams; morphology; structure–property relations

Received 14 March 2015; accepted 1 July 2015
DOI: 10.1002/app.42685

INTRODUCTION

Electrically conductive polymer composites (ECPCs) are produced by the addition of conductive fillers such as carbon black (CB), carbon fiber (CF), metal particles, carbon nanotubes (CNTs), and graphene to an insulating polymer matrix. Their light weight, good chemical resistance, ease of processing, and tunable conductivity make ECPCs an interesting choice for a number of applications, including fuel cell bipolar plates, electromagnetic interference shielding, antistatic parts, and sensors.[1–5]

Until a certain concentration of the conductive filler, the so-called percolation threshold (P_c), polymer composites are insulating, and after that, a spanning cluster of the filler is formed, and the electrical conductivity (EC) starts to increase.[1,3–7] To achieve a desirable conductivity, the filler concentration must be well above P_c. For high-conductivity applications, usually high concentrations of filler are needed; this results in an increase in the composite weight and a decrease in the processability and mechanical properties. The use of multiple fillers and also immiscible polymer blends as polymer matrixes are two strategies used to decrease the amount of filler needed. In polymer composites with an immiscible polymer blend as a matrix, the filler may selectively localize in one phase or within the interphase; therefore, the amount of necessary filler is reduced.[1,8,9]

The foaming of polymers will decrease the density and possibly the production cost as well. On the other hand, the matrix of a foam composite can be considered similar to the matrix of an immiscible polymer blend, in which all of the fillers are located in the polymer phase and often do not enter into the bubbles. The morphology of foam composites, similar to that of immiscible polymer blends, may affect the amount of filler needed to achieve a desirable conductivity. There have been few publications that report the positive effect of foaming on the EC of foam polymer composites.

Yang *et al.*[10] measured the EC of polystyrene (PS)/carbon nanofiber foam composites and reported an insignificant difference between EC and P_c of the foam and solid composites. Motlagh *et al.*[11] used foaming as a way to increase the through-plane conductivity of injection-molded samples. They showed that in composites containing both CB and CF, foaming can increase the through-plane fiber orientation and, thus, the through-plane

conductivity. Thompson *et al.*[12] investigated the effect of foaming on the EC of composites containing CB, CF, and a mixture of them. They reported that foaming in CB and hybrid CF/CB composites led to enhanced conductivity, either in the in-plane or through-plane direction. They observed a reverse trend for the CF composites. Ameli *et al.*[13,14] also investigated the EC, microstructure, and electromagnetic shielding effectiveness of injection-molded CF/polypropylene foam composites. They reported that foaming by nitrogen gas as a physical blowing agent decreases the orientation of fibers along the flow direction and thus increases the through-plane EC of samples. Their results show that the introduction of 25 vol % bubbles reduced P_c from 8.5 to 7 vol % CF. Pelíšková *et al.*[15] foamed ethylene–butylene–acrylate/CB composites. They observed that the foam composites have spherical closed cells at low CB concentrations, but the cells deviate from spherical to oval shape at high CB contents because of their higher viscosity. They reported a reduction in P_c from 10.9 to 5.8 vol % as a result of foaming.

In addition to the experimental methods, computer simulation, a strong technique for studying composite materials, has been frequently used by researchers to investigate the P_c and EC values of solid polymer composites in numerous studies. Computer simulation provides an opportunity to consider the effect of each parameter more precisely and comfortably. Also, its concomitant results can be exploited for the interpretation of experimental results.

Wang and Ogale[16,17] used a computer simulation method to calculate the P_c values of particulate and short-fiber composites. They used a random sequential additional (RSA) process for the distribution of inclusions and, thus, the simulation of the composite structure. Each inclusion was considered to have a hard core and a soft shell; the hard core represented the real inclusion and was not penetrable, but the soft shell was penetrable, and particles with penetrated soft shells were considered electrically connected. In the RSA process, the inclusions are located randomly and sequentially in the simulation sample, but the hard core of each newly added inclusion is not allowed to penetrate the hard cores of the previously existing inclusions.[18] In these two studies, the effects of the particle size, fiber aspect ratio, and soft shell thickness (δ) on P_c were investigated. With the same simulation procedure described previously, Wang and Ogale[19] studied the effect of the fiber orientation on P_c, whereas Dani and Ogale[20] calculated the P_c values of injection-molded composites. Ma and Goa[21] considered the effect of the fiber curvature on the P_c values of composites. They supposed the fibers to be totally penetrable and reported that the fiber curvature caused an increase in P_c. In these studies, finite size scaling was applied to the results of simulations for finite samples to calculate the P_c values of infinite samples.

Zhang and Yi[22] simulated the EC of composites containing carbon-coated glass fibers. They assumed that fibers were totally penetrable and calculated the conductivity by finite element analysis. Grujicic *et al.*[23] used a computer simulation method to predict the conductivity and P_c values of well-dispersed single-walled CNT composites. Johner *et al.*[24] studied electrical tunneling in particulate composites by computer simulation. They used the equilibrium realization of hard spheres to simulate the composite structure. Wang and Ye[25] used a hard core/soft shell model to simulate the structure and piezo resistivity of CNT polymer composites.

The spatial distribution of filler particles in a polymer matrix depends on several parameters, including the filler volume fraction, mixing procedure, filler–filler interactions, and interfacial interactions between the polymer and filler; hence, it is usually very hard to precisely simulate the spatial distribution of inclusions, that is, filler particles, and without experimental data, the real spatial distribution of inclusions is unknown. The RSA and equilibrium realizations of inclusions have been frequently used by researchers to simulate the composite structure. These two methods produce an approximate model for the composite structure, that is, the spatial distribution of inclusions, whereas the real structure of the composite may differ.

As mentioned previously, Ogale and Wang[16,17] used an RSA algorithm to distribute the inclusions and calculate the P_c values of the fiber and particulate composites. They assumed that each inclusion had a hard core and a soft shell. The hard core represented the real size of the inclusion, and the soft shell was half of the effective distance for the electrical conduction between two distinct inclusions. They compared the simulation results with their experimental data and estimated the thickness of the soft shell. The resulting δ was then used to predict the P_c values of the composites with the same type of matrix and filler but with different sizes of filler or production processes. The predictions of the simulation were in agreement with the experimental data. In other words, they assumed that the δ depended only on the matrix and filler type; this assumption showed good agreement with the experimental results. Despite this agreement, the estimated δ was more than two orders of magnitude larger than the tunneling distance for electrical conduction in the polymer composites.[26,27] They explained that this discrepancy was due to the presence of impurities and low-molecular-weight compounds in the composite, which created a multistep conduction mechanism. However, it was clear that the simulated spatial random distribution of inclusions usually differs from the real distribution, and this difference was not considered in the simulations. In fact, the δ was also a correcting parameter for the simulated random distribution and did not only represent the physical distance for electrical conduction.

Louis and Gokhale[28] studied the EC of carbon hollow-sphere composites by experimental methods and computer simulation. They fabricated composite specimens and investigated their microstructure by taking two-dimensional images. To quantitatively characterize the microstructure, they used the nearest neighbor and radial distribution functions. They developed an algorithm to simulate the composite and then used those two microstructure functions to characterize the simulated structures. In their algorithm, the maximum allowed overlap of two distinct spheres was one-tenth of the sphere diameter (d), and overlapped spheres were considered connected.

Nigro *et al.*[29] studied the tunneling conductivity in the polymer composites. They considered attractive potentials between inclusions to account for the surface interactions of fillers to more

accurately simulate the structure of the polymer composites. In this study, the equilibrium distribution of attractive hard spheres was obtained by a metropolis algorithm.

The use of computer simulation to estimate the effect of foaming on the P_c values of ECPCs has not been reported. In this study, computer simulation based on the RSA method was used to construct the structure of foamed and solid PS composites and to estimate their P_cs. The effects of the fiber aspect ratio, bubble volume fraction, and bubble radius (R) on the P_c and accessible fiber fraction were studied by the RSA method. Also, the EC and P_cs of both the solid and foam PS composites containing various amounts of CF and CNTs were determined experimentally to evaluate the simulation results.

SIMULATION PROCEDURE

The spatial distribution of fillers is not uniform in foam composites because of many involved factors.[1] Fillers do not penetrate into the bubbles.[12] In other words, bubbles have a volume exclusion effect for fillers, as shown later by scanning electron microscopy (SEM) images in the Experimental section. Foaming might also have had other effects on the distribution of fillers; the concentration of fillers might have been higher near the boundary of the bubbles rather than other locations in the matrix because of the growth of bubbles and, consequently, the flow of matrix and fillers around the bubbles.[11] We assumed that only in foams with large bubbles (relative to the size of fillers) could the distribution of the fillers be significantly changed. The spatial distribution of inclusions in the foam composites with small bubbles was assumed to be similar to that in solid composites because small bubbles changed the distances between inclusions smoothly and uniformly. In other words, in a foam composite with small bubbles, if one considers filler volume fraction with respect to the total volume of the composite, the EC of the foam composite is expected to be equal to the EC of the counterpart solid composite with the same concentration. Equally, when the concentration of filler is considered with respect to the solid part of a foam composite, the EC of the foam composite with small bubbles will be less than the EC of its counterpart solid composite with the same concentration.

In this study, the volume exclusion effect of the bubbles in which fillers do not penetrate into the bubbles, was postulated as the major characteristic for the foam composite. Only foams with large bubbles were considered in the simulation. In the simulation procedure, cylinders and spheres as fibers and bubbles were distributed uniformly in a cube with the well-known RSA process. All of the cylinders and spheres were the same in size. Each cylinder was defined by five parameters: three to determine the coordinates of a point on the axis of the cylinder and two to determine the orientation angle of the axis. Also, three parameters were necessary to define a bubble, that is, the coordinates of the bubble center. For the simulation, all of the spheres were distributed in the cube first, and then, the cylinders were added. This is a suitable sequence for distributing cylinders and large spheres by the RSA method; this method causes a maximal volume exclusion effect by the spheres on the cylinder position, and it is consistent with the real structure of a foam composite with large bubbles. In fact, if the opposite sequence is used, that is, first cylinders and then spheres are distributed, there will not be enough free space between the cylinders to insert large spheres. The cylinders and spheres were assumed to be impenetrable. In a real composite, a cylinder (fiber or CNT) does not penetrate into spheres (bubbles) or other cylinders. Thus, this was considered in the simulation. The bubbles were assumed to be impenetrable in each other because the volume fraction of the entered bubbles was much easier to control in this way. If the minimum distance between the two cylinders was smaller than the δ, the two fibers were assumed to be connected for electrical connection. In other words, the cylinders were considered to be semipenetrable with a hard impenetrable core and a penetrable soft shell. The hard core d was the same as the fiber or CNT d, and the δ was half of the maximum distance required for electrons to transfer between cylinders. In Figure 1, the assumed model for conductive fibers (cylinders) and the pictures of some of the simulated foam composite structures are illustrated.

A set of several interconnected cylinders formed a cluster in the simulated cube. In the simulation algorithm, each added cylinder was assigned a unique cluster number. These cluster numbers for n cylinders entered a one-dimensional array with n members. n was the total number of cylinders, and the ith element of the array represented the cluster number of the ith entered cylinder. If the newly entered cylinder to the cube connected to other cylinders so it became a member of one or more already existing clusters, the cluster array was updated to assign the same cluster number to all of these interconnected cylinders.

After the addition of each cylinder, the cube was checked, and if there was a spanning cluster of the cylinders that connected all six walls of the cube together, the addition of the cylinders was terminated, and the volume fraction of the cylinders was calculated as P_c. The periodic boundary conditions were not applied. The single-cube boundary condition was used, in which the hard cores of the cylinders were not allowed to penetrate into the walls of the cube. The validity of this boundary condition was verified with two concentric cube boundary conditions; this is discussed with the simulation results. If the soft shell of a cylinder penetrated into one of the walls of the cube, the cylinder was assumed to have electrical connection with that wall; by considering whether the fibers had electrical connections with the walls, we found it easy to determine whether a spanning cluster of fibers was formed in the sample.

In fact, most composites are infinite in size and P_c, for an infinite size composite is only a unique value. If the composite size is not large enough, P_c decreases with increasing the size of the composite. Because a finite cube size was used to simulate the composite structure and obtain P_c, every run of the simulation returned a different value, and their average was considered as the finite size P_c. Finite size scaling was applied to calculate P_c for the equivalent infinite size composite. From several proposed equations for the finite size scaling of percolation systems, eq. (1) was selected and used. In this equation, P_c, P_{ave}, and Δ are the asymptotic percolation concentration for an

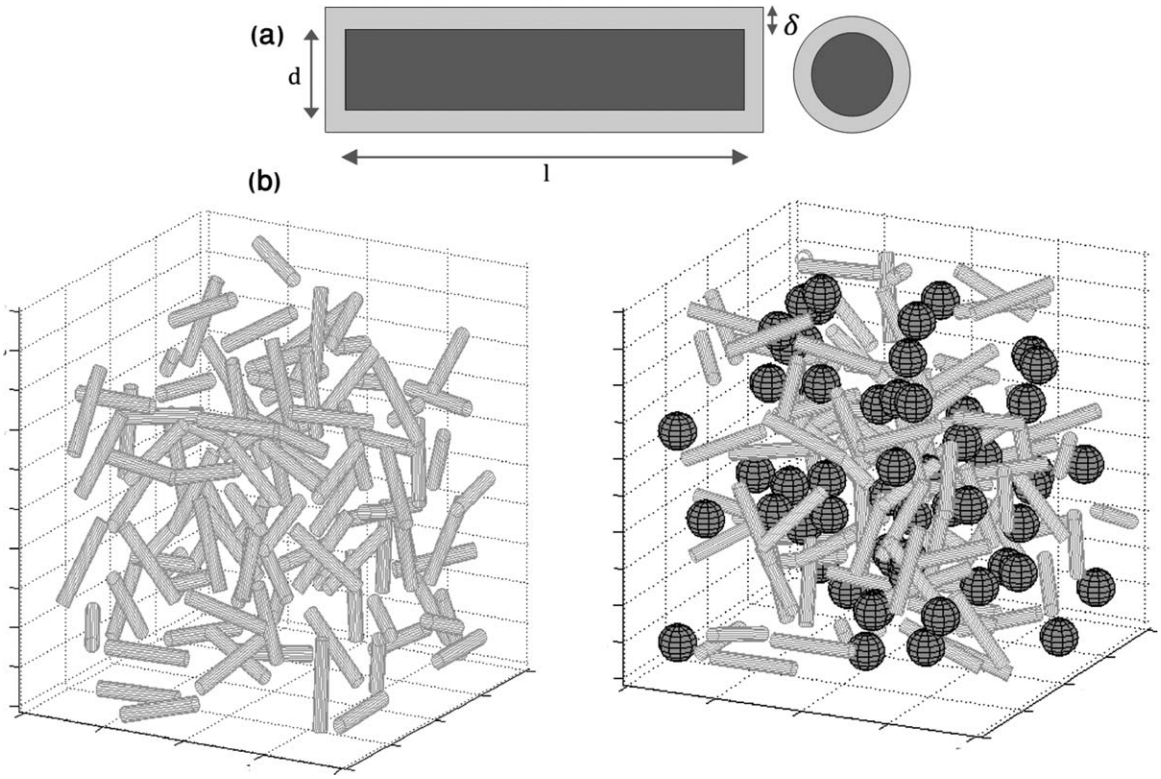

Figure 1. (a) Assumed soft shell and hard core structure of the fiber and (b) simulated structure for (left) a solid composite containing 3 vol % fibers and (right) a 3 vol % foam composite containing 3 vol % fibers. The aspect ratio of all of the fibers was 6.

infinitely large system, average P_c for a finite system with a side length (L), and the standard deviation (STD) of the resulting thresholds for a composite with L, respectively:[30]

$$|P_c - p_{ave}| \approx \Delta \quad (1)$$

To determine P_c of an infinite size composite, the true P_c, a simulation was run several times with the same parameters for cubes with different sizes to obtain P_c. The average and STD of the resulting P_cs for several boxes were obtained. According to eq. (1), by fitting a line to P_{ave} versus Δ, one can calculate P_c by extrapolating the line to $\Delta = 0$ for an infinite size sample. For example to calculate P_c of a composite containing fibers with length (l) = 4.65, $d = 0.775$, and $\delta = 0.125$, the simulation was run for four cube ls of 14, 17, 20, and 24 several times, and P_{ave} and Δ were calculated for each of them. Figure 2(a) shows P_{ave} versus the number of simulation iterations for these composites, and Figure 2(b) shows P_{ave} versus Δ for these finite composites. The intercept provided P_c for the infinite size composite. A P_c value of 0.113 and a fitting correlation coefficient (R^2) values of 0.995 were obtained. The obtained P_c was in good agreement with the P_c value of 0.115 reported by Ogale and Wang[17] for a composite with the same fiber dimensions. This harmonious result also indicated the effectiveness of eq. (1) for finite size scaling for continuum percolation systems, although it was first proposed for lattice percolation. In the rest of this article, unless otherwise mentioned, the given P_cs are for infinite size samples obtained through the procedure explained previously.

SIMULATION RESULTS

In this part of the study, the simulation procedure was implemented with the foam and solid composites. The boundary conditions, cube size, R, bubble volume fraction, fiber aspect ratio, and δ were changed as parameters of the simulation.

In the next part of the study, the simulation results were evaluated by the experimental results.

Effect of the Boundary Conditions

Because boundary fibers have a major effect on the existence of a spanning cluster, it might have been possible that the considered single-cube boundary condition influenced the calculated final P_c. To investigate this effect, the simulation was run with different boundary conditions for four cube sizes. In this boundary condition, two-concentric cubes were considered where the fibers and bubbles were distributed in the inner/outer cubes, but only the fibers in the inner cube took part in the formation of the percolating cluster. The l values of the inner cube were selected as 14, 17, 20, and 24, and the l of the outer cube in each case was the l of the inner cube plus two times the fiber l. Figure 3 shows the results of the boundary condition effect for fibers with $l = 4.65$, $d = 0.775$, and $\delta = 0.125$. As observed, the P_cs for the single-cube boundary condition were lower than those of the two concentric cube boundary conditions. However, as the size of the cube increased, the effect of the boundary condition decreased. Finally, for an infinite size cube, the difference became relatively insignificant.

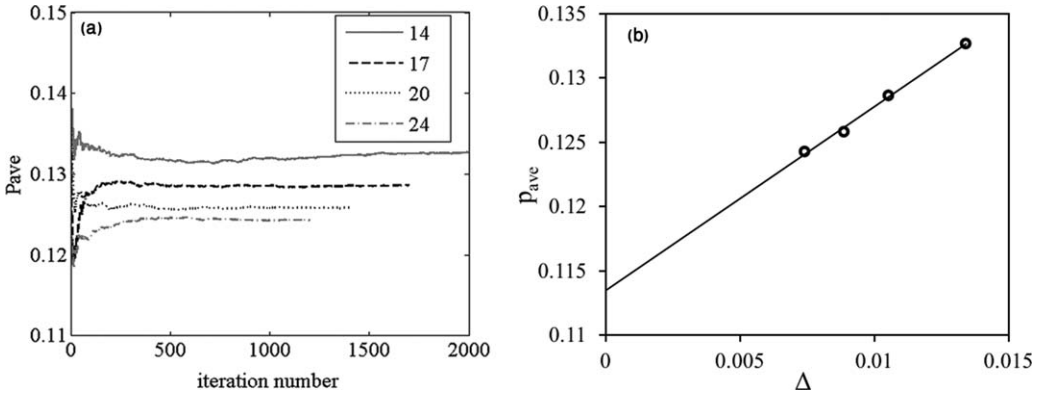

Figure 2. (a) P_{ave} against simulation iteration and (b) P_{ave} against Δ. For solid composites, fiber $l = 4.65$, fiber $d = 0.775$, and $\delta = 0.1125$.

Effect of Foaming on P_c

The explained RSA-based simulation was used to obtain the P_c values of the solid and foam composites. The parameters included δ, fiber aspect ratio (l/d), R, and bubble volume fraction.

The effect of the bubble volume fraction is shown in Figure 4(a) with a plot of P_c against Δ for some finite composites containing fibers with $l = 4.65$, $d = 0.775$, $R = 2$, and two bubble volume fractions of 15 and 20. As observed for all of the cube sizes, the solid composite had a lower P_c than the foam composite. With increasing cube size, the difference between the P_c values of the solid and foam composites decreased. By finite size scaling, P_cs of 0.113, 0.116, and 0.118 were calculated for an infinite size solid, 15% foam, and 20% foam composites, respectively. These three values for P_c were based on the volume of the solid part of the foam composites, that is, the ratio of the fiber volume to the matrix volume. As the results show, a slightly higher P_c was observed for the composite with a higher bubble volume, but the differences were negligible; however, when the P_cs were calculated as the ratio of the fiber volume to the total composite volume, we found that P_c declined with the bubble content. For instance, P_c for the composite, containing 15 vol % bubbles on the basis of the total volume of was $0.85 \times 0.116 = 0.099$; this was smaller than the value of 0.113 for the solid composite.

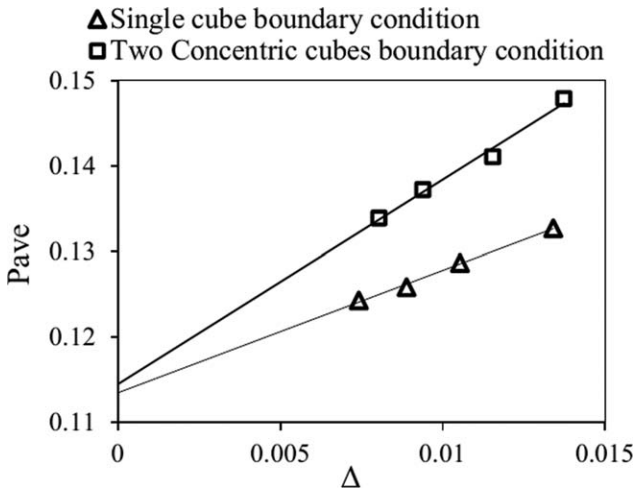

Figure 3. Effect of the boundary conditions on P_c. Fiber $l = 4.65$, $d = 0.775$, and $\delta = 0.1125$.

The effect of the bubble volume fraction was also evaluated for a larger δ. According to Figure 4, an increase in δ increased the number of connected fibers and led to a decrease in P_c. Figure 4(b) shows the results of simulations for solid and foam composites containing fibers with $l = 4.65$, $d = 0.775$, and $\delta = 0.3$. We predicted values of 0.047, 0.047, 0.049, 0.051, 0.052, and 0.054 for P_c's of the solid and 5, 10, 15, 20, and 25% foam composites, respectively. These reported P_cs are based on the matrix volume.

The P_cs of the composites containing fibers with an aspect ratio of 12 were also calculated by the application of a similar procedure. In Figure 5, the results of the simulations for fibers with aspect ratios of 6 and 12 are depicted. For the aspect ratio of 12, R was 2.5 ($R/l = 0.27$), and for the aspect ratio of 6, R was 2 ($R/l = 0.43$). For all cases, the obtained P_c of the foam composite was larger than that of the solid composite, but the difference was negligible. In most cases, the difference between the P_cs of the 15% foam composite and the solid composite was less than 3%.

The effect of R on P_c was shown in Figure 6 for the composites with a 15 vol % bubble fraction. Here, finite size scaling was not applied, and instead, a large cube size containing about 100,000 inclusions was simulated with a single run of simulation for each R, and the obtained P_c was reported as P_c. As we observed, a change in R caused little variation in P_c. It seemed that as the bubbles got smaller, the effect of R became more considerable.

EXPERIMENTAL

Materials and Experimental Method

To experimentally investigate the effect of foaming on the electrical behavior and to validate the simulation results, several solid and foam samples were made. PS (GPPS1540 Tabriz Petrochemical Co.) was selected as the matrix. PS as an amorphous polymer was used to exclude the effect of the crystallinity of a semicrystalline matrix on the interpretation of the results. The properties of semicrystalline polymers depend on the degree of crystallinity, which is affected by the processing conditions, the presence of fillers, and probably foaming. Therefore, a

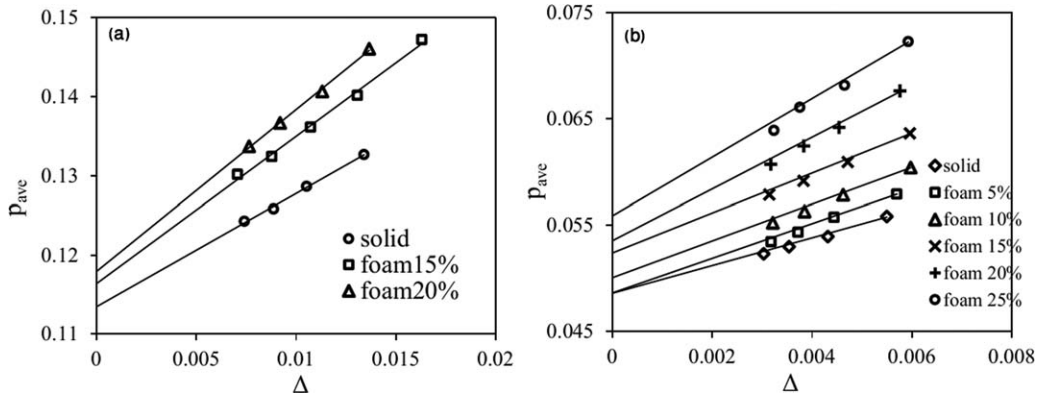

Figure 4. P_{ave} against Δ for finite size solid and foam composites (fiber $l = 4.65$, $d = 0.775$, and bubble radius = 2) for (a) $\delta/d = 0.145$ and (b) $\delta/d = 0.39$.

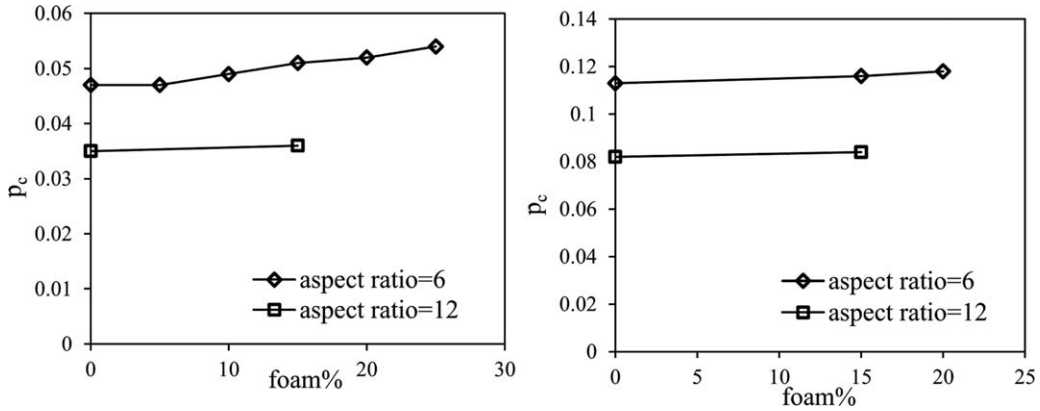

Figure 5. P_c for the composite containing fibers with (left) $\delta/d = 0.39$ and (right) $\delta/d = 0.145$.

semicrystalline matrix led to the complexity of morphology and difficulty in the interpretation of the experimental results after foaming. The conductive fillers used in this study included a polyacrylonitrile (PAN)-based CF (AGM-94-Asbury) and multiwalled CNTs (Chengdu, china). The properties of these two fillers are given in Table I. *P*-Toluene sulfonyl semicarbazide (TSSC) was used as a chemical blowing agent. TSSC releases nitrogen gas at a temperature range of 228–235°C with a gas yield of 140 to150 mL/g.

CF and CNTs under various concentrations were mixed with PS in a 50-cc Brabender internal mixer at 200°C and 60 rpm for 12 min. First, PS was added to the mixer to melt. After 4 min, the CFs or CNTs were introduced into the melt, and mixing was continued for another 6 min. To prepare compounds for the foam composites, 0.5 wt % TSSC was added to the melt during the last 2 or 3 min of the mixing time to minimize TSCC decomposition in this stage. The prepared compounds were then compression-molded into 3.5 mm thick sheets at 220°C and 50 bar in a temperature-controlled hydraulic press. The preheating time was 5 min for the solid and 3 min for the foam composites. Then, preheating pressure was applied to the mold for 2 min, and the mixture was cooled under pressure. For the

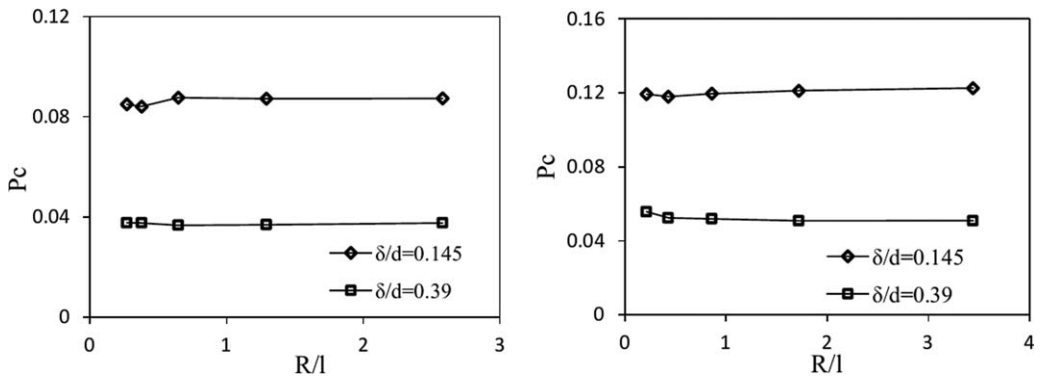

Figure 6. P_c for the composite containing fibers with (left) $l/d = 12$ and (right) $l/d = 6$.

Table I. Physical Properties of the Used CF and CNTs

CF	
EC (S/cm)	625
Fiber *d* (μm)	7.5
Fiber *l* (μm)	5000
Residue, 1000°C, 30 min, air (wt %)	<10
Multiwalled CNTs	
Outer *d* (nm)	10–20
Purity (wt %)	>85
l (μm)	30–100
Surface area (m^2/g)	>165
Ash, 1000°C, 30 min, air (wt %)	2

foam samples, the volume of the material was calculated to be insufficient to completely fill the mold and leave free space for the cells to grow. The CF compounds were prepared at 5, 8, 11, 15, and 20 wt % CF, whereas the CNT compounds contained 1.5, 2, 3, and 5 wt % CNTs. Specimens were cut from the molded sheets for measurements and analysis.

The four-probe method was used to measure the in-plane (along the *l*) EC of the rectangular specimens (dimensions = 45 × 5.8 mm^2), in a manner similar to the method explained by Motlagh *et al.*[31] The *R* distribution was obtained by electron microscopy. The CF *l* distribution was determined by optical microscopy. To measure CF *l*, 5 and 15 wt % CF solid composites were pyrolyzed at 500°C in a tubular furnace under a nitrogen purge. The remaining ash and fibers were dispersed in methanol and dried on microscope slides to obtain images by an optical microscope and measure the fiber *l*. The distributions were determined on the basis of at least 200 bubbles and 400 fibers. For the qualitative evaluation of CNT dispersion and distribution, thin films were prepared by hot pressing of a small amount of the nanocomposites for optical microscopy. Also, Raman spectroscopy was used to further investigate the distribution/dispersion of the CNTs in the composites. The laser excitation wavelength of the Raman spectrometer was 785 nm with a spectral resolution of less than 3 cm^{-1} and a confocal depth resolution of 2 μm. Raman spectra were collected on areas of 10 × 10 μm^2 at three different locations of the as-received CNTs and the selected solid and foam composites.

Experimental Results

Figure 7 shows the SEM images of the CF and CNT composites. For the CF composite, fiber pullout was observed at the fracture surface because of poor interfacial adhesion between the fibers and the matrix. For the foam CF composite, the majority of fibers did not penetrate into the bubbles; this supported the excluded volume assumption. In addition, for both CF and

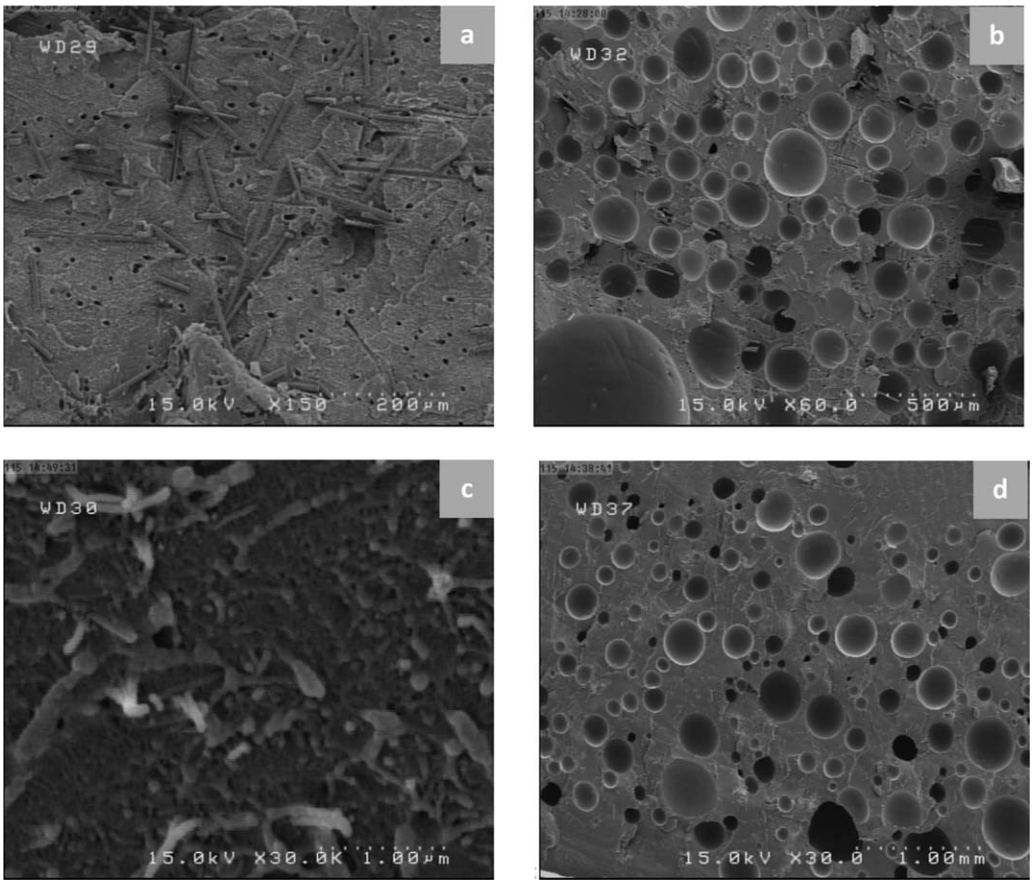

Figure 7. SEM images of the (a) solid composite containing 5 wt % CF, (b) 15 vol % foam composite containing 5 wt % CF, (c) solid composite containing 5 wt % CNTs, and (d) 15 vol % foam composite containing 1.5 wt % CNTs.

Table II. *R* and Fiber *l* Values of Some of the Foamed and Solid Composites

		Bubble *d*			
Foam specimen	Foaming percentage	$\bar{D}$ (μm)	$(\bar{D}^3)^{1/3}$	*D* STD	*N*
CF 5 wt %	15	117.5	130	39	130
CF 5 wt %	30	133	166	62	125
CF 15 wt %	15	122	142	50	100
CF 15 wt %	30	170.5	220	97.5	53
CNT 1.5 wt %	15	146	191.5	85	41
CNT 1.5 wt %	30	166.5	204.5	82.5	67
		Fiber length			
Solid specimen	*l* (μm)	*l* STD	Aspect ratio		
CF 5 wt %	255	146	36.5		
CF 15 wt %	148.3	63.7	21.2		

D = number average diameter, $(\bar{D}^3)^{1/3}$ = volume average diameter of cells.

CNT foam composites, the bubbles were spherical with a nonuniform size distribution. Some characteristics of the cell morphology obtained from the SEM micrographs are given in Table II. As shown for the CF composites, an increase in either the foaming percentage or filler content increased the average *R* and decreased the number of bubbles per unit volume (*N*). For the CNT composites, an increase in foaming percentage led to an increase in *R* and a decrease in *N*. *R* and *N* were affected by several parameters, including the viscosity, nucleation effect of the filler, and filler–filler and filler–matrix interactions. The results of fiber *l* measurements from optical microscopy are also demonstrated in Table II. An increase in the fiber content from 5 to 15 wt % led to a significant decrease in the fiber *l*. Higher viscosity and fiber–fiber interactions were responsible for the breakdown of fibers in the mixing and molding processes. The optical image of the thin film of the 1.5 wt % CNT solid composite in Figure 8 shows a relatively poor dispersion and distribution state of the CNTs and the appearance of some agglomerates.

Figure 9 displays the Raman spectra of the CNTs [Figure 9(a)], 1.5 wt % CNT/PS solid composite [Figure 9(b)], and also 1.5 wt % CNT/PS foam composite [Figure 9(c)]. Two strong peaks were observed for CNTs at 1303 and 1600 cm^{-1}; the latter, namely, the G band, was assigned to the tangential vibrations of the C atoms, and the former, the so-called D band, was related to defects in the nanotubes. As shown in Figure 9(a), the D-band intensity (I_D) was relatively strong; this was probably due to the defects in the industrial grade CNTs used in this study. According to Figure 9, the G bands in the solid and foam composites did not show a noticeable shift compared to that in the as-received CNTs. The G-band intensity (I_G) is usually used to evaluate the concentration of nanotubes in a polymer matrix;[33] (shown later), but here, the PS aromatic ring (C=C) also showed a strong peak around 1600 cm^{-1}, which overlapped the CNTs' G band.[32] Therefore, in this study, the relative I_D was used to evaluate the concentration of the CNTs. For the selected samples mentioned previously, Raman spectroscopy was run at three different points for each specimen, and the obtained spectra were associated with the uniformity of the CNT distribution. We normalized the I_D value for each composite by dividing I_D by the sum of I_D and the intensity of PS characteristic peak at 999 cm^{-1} (I_P), that is

$$I_D^* = [I_D/(I_D + I_P)] \quad (2)$$

The normalized D band intensity (I_D^*), given in Figure 9(b,c), was proportional to the density of nanotubes in each specimen. As shown, I_D^* for either the solid or foam composite was not the same at the three locations; this could have been due to the nonuniform distribution of CNTs and the presence of bundled and agglomerated CNTs. This finding was in agreement with the optical microscopy image of the CNT solid composite (Figure 8). The consistency of the optical microscopy results with Raman spectra was also reported by other researchers.[33] The I_D^* values also suggest that the foam composite had a better distribution for CNTs because of less deviation among the three locations.

The ECs of the CF and CNT composites are shown in Figure 10. EC is plotted against the filler volume fraction on the basis of both the matrix volume and the total volume of the composite. The universal percolation model, shown next, was fitted on all of the series of conductivity data to estimate P_c for the solid and foam composites:

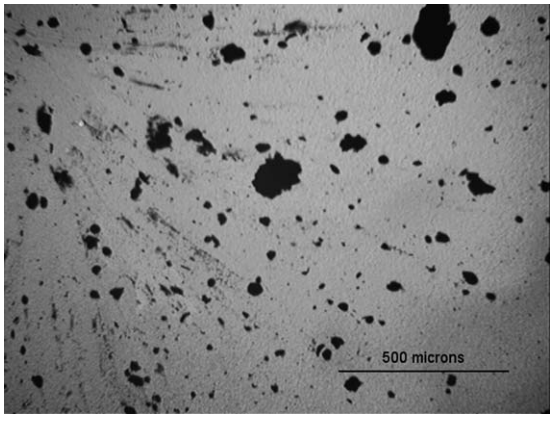

Figure 8. Optical microscopy image of the 1.5 wt % CNT composite.

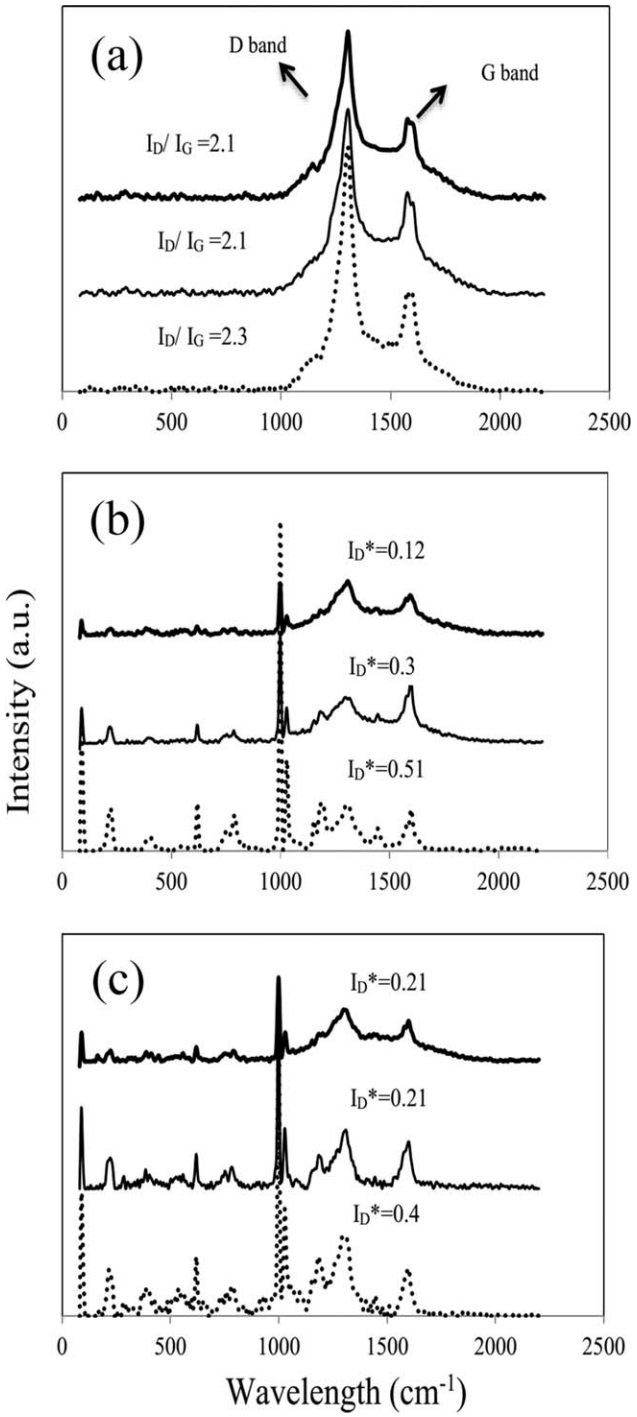

Figure 9. Raman spectra of the (a) MWCNTs, (b) 0.7 wt % CNT solid composite, and (c) 0.7 wt % CNT foam composite at three different positions.

$$\sigma = \sigma_0 (p - P_c)^t \quad (3)$$

where σ, σ_0, p, P_c and t are electrical conductivity of composite and filler, filler volume fraction, percolation threshold and critical exponent, respectively. The best fitted parameters are given in Table III. As shown in Figure 10(a) and Table III, when the volume fraction was determined with respect to the matrix volume, foaming decreased EC and increased P_c of the CF composites. With increasing degree of foaming from 15 to 30 vol %, EC increased, and P_c decreased. This could have been due to the change in the fiber orientation/distribution during foaming.[11–14] When the volume fraction was calculated on the basis of the total volume of the composite, that is, the bubble volume was considered, foaming at a level of 30 vol % improved EC of the CF composites and, consequently, decreased P_c, but the conductivity of 15 vol % foam still remained smaller than that of the solid composite. For the CNT foam composites, a trend similar to that of the CF composites (30 vol % foam) was observed, as shown in Figure 10(b) and Table III, however, with a stronger effect of foaming. By considering the CNT volume fraction with respect to the matrix volume, we observed that foaming caused small changes in EC of the CNT composites. When the total volume fraction was considered, ECs of both the 15 and 30 vol % foam composites were better than that of the solid composite. In conclusion, in both the CF and CNT composites, the 30% foam composites showed better conductivity than the 15% foam composites; this could have been a result of the filler reorientation/redistribution induced by foaming.[11–14]

COMPARISON OF THE SIMULATION AND EXPERIMENTAL RESULTS

The average value of R, fiber l, and obtained values of P_cs from the experimental results for the solid and foam CF composites at two levels of 15 and 30 vol % were used as inputs for the simulation. The output as P_cs were used to evaluate the simulation results.

According to Table II, 5 wt % (3 vol %) CF composites contained fibers with an average l of 252 μm and bubbles with weighted average ds of 130 and 166 μm for the 15 and 30 vol % foams, respectively. The simulation was run with these mentioned parameters at a scale of 0.1. All of the composites contained fibers with $l = 25.2$ and $d = 0.7$, and for foam composites and bubbles with R values of 6.5 and 8.3 for the 15 and 30 vol % foams, respectively. To choose an appropriate value for δ, a simulation was run for the solid composites with several values of δ; the corresponding P_c to each δ was obtained. Among the different values of δ, the one that returned the same percolation value measured experimentally; that is, 0.018 was selected as the appropriate δ for the rest of simulations. As mentioned in the Introduction section, researchers of previous studies[16,17] also used soft shell manipulation to obtain acceptable output from their simulation runs for solid composites. Therefore, a δ of 0.25 was determined as the most appropriate δ with the help of the experimental results. To simplify the modeling, the simulation was run only one time for a large cube size with a dimension of 450 × 450 × 450. We found from our simulation runs that this cube size was large enough to prevent multiple time-consuming steps for various small cube sizes. Therefore, finite size scaling was not applied here.

The P_c values for the solid and 15 and 30 vol % foam CF composites were obtained from computer simulation as 0.0180, 0.0181, and 0.0181, respectively. These values were with respect to the matrix volume fraction. Like the results of the simulation section, the P_cs of the foam composites were approximately

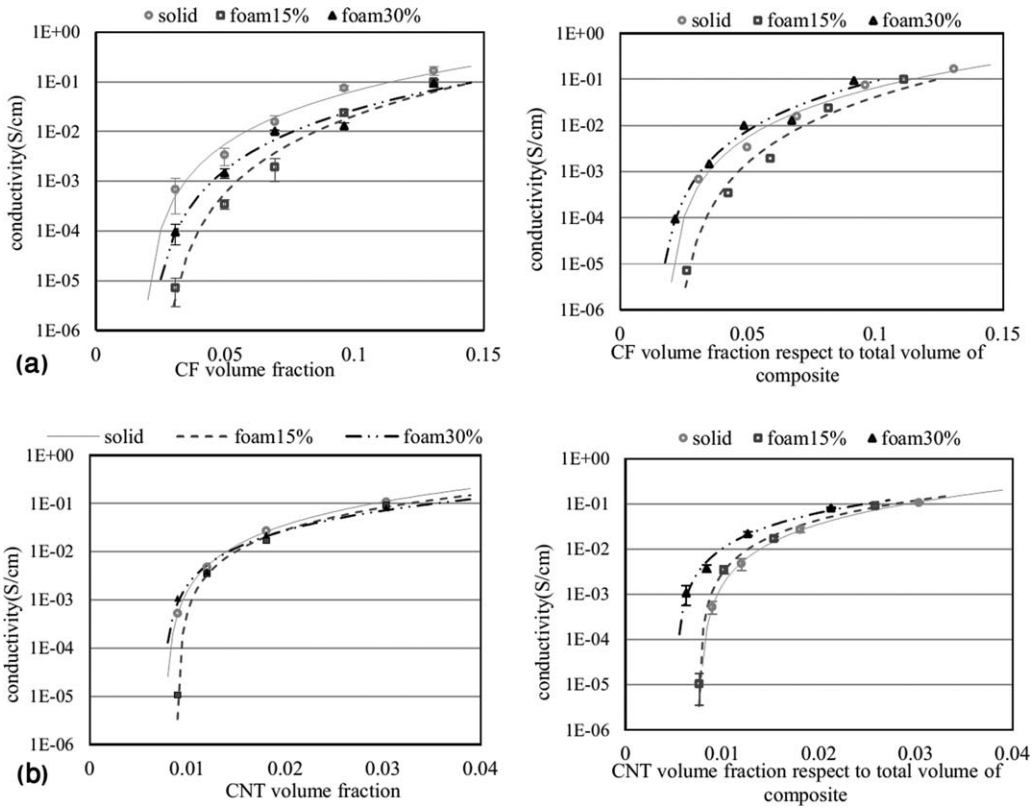

Figure 10. In-plane EC of the solid and foam composites: (a) CF composites and (b) CNT composites.

similar to the P_c of the solid composite but were different from the experimental results given in Table III. These differences could have been due to the change in fiber orientation/distribution during foaming; this was not considered in the simulation. The assumption of having the same filler morphology for the foam composite and the solid composite was not true. Because the CNTs were similar to the CFs, we expected that similar results would be observed for the simulation of the CNT composites; that is, there would be similar P_cs for the solid and foam composites. Table III shows that the P_c of the CNT foam composite at 15 vol % foam was higher than that of the solid composite, but a higher degree of foaming (e.g., 30 vol %) decreased P_c. Therefore, the simulation results show that when the orientation and distribution of fillers did not change during foaming, a good agreement with the experimental results was observed. That is, for the solid composites when the composites were foamed, the change in the filler orientation/distribution caused disagreement between the simulation and experimental results.

Table III. Parameters of Percolation Model for the Foam and Solid Composites

	σ_0	P_c	t
CF composites			
Solid CF composites	400	0.018	3.3
15% foam CF composites	370	0.023	3.7
30% foam CF composites	200	0.020	3.4
CNT composites			
Solid CNT composites	128	0.0077	1.86
15% foam CNT composites	52	0.0089	1.67
30% foam CNT composites	32	0.0075	1.61

σ_0 = filler volume fraction, P_c = critical exponent.

In general, the inharmonious results between the experimentally obtained P_cs of the CF foam composite and the simulated values, especially at 15 vol %, were due to the differences in the morphology of the real composites with the morphology postulated in the simulated composites. The size distribution of the fibers and bubbles, the possible preferred orientation of the fibers in compression molding, and the difference in the spatial distribution of the fibers in the real composites may have caused this unexpected outcome. Also, changes in the concentration, orientation, and thus, the connectivity of the fibers near the surfaces of the bubbles during bubble growth were not considered in the simulation. As mentioned before, in the simulation approach, at first all bubbles were introduced in the cube, and then, the fibers were added by the RSA method. This manner of modeling led to a maximal spatial inhibition of bubbles in the positioning of the fibers within the composite; this might have produced a composite with a different spatial distribution of fillers than that of a real composite. However, the results of the simulation were qualitatively in agreement with the reported results, in which the selective localization of fillers in one phase decreased P_c and, in turn, increased EC.[1,8,9]

In addition, to obtain P_c by simulation, the accessible fractions (χs) of the fibers in solid and foam composites were also calculated by simulation. χ is the concentration of conductive fillers

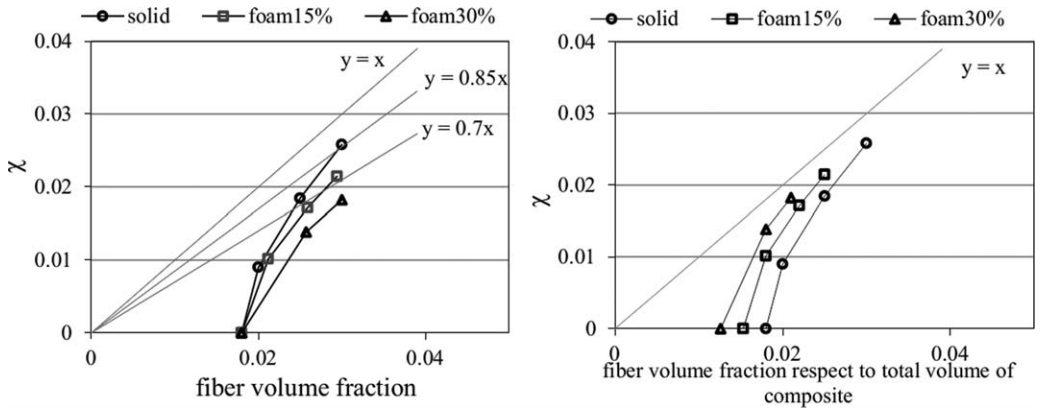

Figure 11. Accessible fraction (χ) against the fiber volume fraction obtained by the simulation for the experimentally prepared CF composite.

taking part in the formation of a conducting spanning cluster throughout the composite. Fillers that are not involved in the formation of a spanning cluster do not take part in electrical conduction. In addition, all members of the spanning cluster do not provide electrically conductive pathways for electrons because of the presence of dead ends. The purpose of calculating χ was to compare the EC of the solid and foam composites qualitatively because no direct relation was available between the conductivity of the composite and its χ.

The diagrams of the χ values of the solid and foam composites against the fiber volume fraction are shown in Figure 11. In both diagrams, χ was in respect to the total volume of the composite in the case of the foam composites. In the vicinity of P_c, χs of the solid and foam composites showed a small difference, but relatively far from P_c, χ of the solid composite was greater than that of the foam composite. When the fiber volume fraction increased, more fibers became members of the continuous percolating cluster, and finally, all of them made a single large cluster. In this case, the trend lines became tangential to the lines $\chi = p$, $\chi = 0.85p$, and $\chi = 0.7p$ for the solid and 15 and 30 vol % foam composites, respectively. The slopes present the volume percentage of the solid in the composites. Therefore, we suggested that near P_c, foaming had little effect on EC, and as the filler volume fraction increased, the effect of foaming became more significant.

CONCLUSIONS

The effect of foaming on the electrical percolation behavior of the fiber composites was investigated by means of computer simulation and experiments. The RSA process was used to simulate the structure of the solid and foam composites. The validity of the simulation results was confirmed by comparison to the results of previous studies. The simulation results show that P_c decreased with increasing fiber aspect ratio and δ, whereas it increased with bubble volume fraction and did not change with R. The simulation runs for several composites containing bubbles and fibers with different sizes showed that the P_cs of the foam composites with bubbles not much smaller than fibers were approximately equal to the P_cs of the solid counterparts.

The effects of foaming on the EC of several CF and CNT composites were also experimentally studied. For the CF composites, the conductivity declined, and P_c increased with foaming, whereas no significant change was observed for the CNT composites. However, for both fillers and at several concentrations, the EC of 30% foam was more than that of the 15% foam; this could have been due to the filler reorientation/redistribution during foaming. Moreover, we observed that when the volume fraction of the filler was observed with respect to the total volume of the foam composite, foaming, to some extent, enhanced the EC of CF and CNT composites compared to their solid counterparts. Only for the 15% foam CF composite did foaming have an adverse effect on its EC.

The simulation procedure was evaluated by the experimental results. The morphological characteristics of the composites, such as the fiber l and R, measured experimentally were used to run the simulation to evaluate its agreement with the experimentally determined P_c. There was good agreement for the solid composite. However, the simulation results show nearly no changes in P_c with foaming; this was in contrast to the experimental results. This was due to the use of the RSA approach and the random distribution of fibers and bubbles in the simulation, whereas the experimental results reveal that foaming may have induced the distribution of the filler particles to form a more efficient network.

REFERENCES

1. Huang, J. C. *Adv. Polym. Technol.* **2002**, *21*, 299.
2. Zhang, W.; Dehghani-Sanij, A. A.; Blackburn, R. S. *J. Mater. Sci.* **2007**, *42*, 3408.
3. Spitalsky, Z.; Tasis, D.; Papagelis, K.; Galiotis, C. *Prog. Polym. Sci.* **2010**, *35*, 357.
4. Potts, J. R.; Dreyer, D. R.; Bielawski, C. W.; Ruoff, R. S. *Polymer* **2011**, *52*, 5.
5. Sengupta, R.; Bhattacharya, M.; Bandyopadhyay, S.; Bhowmick, A. K. *Prog. Polym. Sci.* **2011**, *36*, 638.
6. Sahimi, M. Applications of Percolation Theory; CRC: Boca Raton, FL, **1994**.
7. Balberg, I. *Carbon* **2002**, *40*, 139.
8. Cayla, A.; Campagne, C.; Rochery, M.; Devaux, E. *Synth. Met.* **2011**, *161*, 1034.
9. Tan, Y.; Song, Y.; Cao,Q.; Zheng, Q. *Polym. Int.* **2011**, *60*, 823.

10. Yang, Y.; Gupta, M. C.; Dudley, K. L.; Lawrence, R. W. *Adv. Mater.* **2005**, *17*, 1999.
11. Motlagh, G.; Hrymak, A.; Thompson, M. *Polym. Eng. Sci.* **2008**, *48*, 687.
12. Thompson, M.; Motlagh, G.; Oxby, K.; Hrymak, A. *J. Appl. Polym. Sci.* **2010**, *115*, 646.
13. Ameli, A.; Jung, P.; Park, C. *Carbon* **2013**, *60*, 379.
14. Ameli, A.; Jung, P.; Park, C. *Compos. Sci. Technol.* **2013**, *76*, 37.
15. Pelíšková, M.; Piyamanocha, P.; Prokeš, J.; Varga, M.; Sáha, P. *Synth. Met.* **2014**, *188*, 140.
16. Wang, S.; Ogale, A. *Compos. Sci. Technol.* **1993**, *46*, 93.
17. Ogale, A.; Wang, S. *Compos. Sci. Technol.* **1993**, *46*, 379.
18. Torquato, S. Random Heterogeneous Materials. Microstructure and Macroscopic Properties. Interdisciplinary Applied Mathematics. *16*; Springer: New York, **2002**.
19. Wang, S.; Ogale, A. *Compos. Sci. Technol.* **1993**, *46*, 389.
20. Dani, A.; Ogale, A. *Compos. Sci. Technol.* **1996**, *56*, 911.
21. Ma, H.; Gao, X. L. *Polymer* **2008**, *49*, 4230.
22. Zhang, T.; Yi, Y. *J. Appl. Phys.* **2008**, *103*, 014910.
23. Grujicic, M.; Cao, G.; Roy, W. *J. Mater. Sci.* **2004**, *39*, 4441.
24. Johner, N.; Grimaldi, C.; Balberg, I.; Ryser, P. *Phys. Rev. B* **2008**, *77*, 174204.
25. Wang, Z.; Ye, X. *Nanotechnology* **2013**, *24*, 265704.
26. Balberg, I.; Azulay, D.; Toker, D.; Millo, O. *Int. J. Mod. Phys. B* **2004**, *18*, 2091.
27. Balberg, I. *Phys. Rev. Lett.* **1987**, *59*, 1305.
28. Louis, P.; Gokhale, A. *Acta Mater.* **1996**, *44*, 1519.
29. Nigro, B.; Grimaldi, C.; Miller, M.; Ryser, P.; Schilling, T. *J. Chem. Phys.* **2012**, *136*, 164903.
30. Stauffer, D.; Aharony, A. *Introduction to Percolation Theory; Taylor & Francis:* London, UK, **1992**.
31. Motlagh, G.; Hrymak, A.; Thompson, M. *J. Polym. Sci. Part B: Polym. Phys.* **2007**, *45*, 1808.
32. McCreery Research Group. National Institute for Nanotechnology, University of Alberta. Standard Spectra. Available at http://www.chem.ualberta.ca/~mccreery/ramanmaterials.html. Accessed on June 26, 2015.
33. Du, F.; Sconga, R. C.; Zhou, W.; Brand, S.; Fischer, J. E.; Winey, K. I. *Macromolecules* **2004**, *37*, 9048.